Spatial Vision, Vol. 12, No. 3, pp. 267–285 (1999)

Spatial pattern summation is phase-insensitive in the fovea but not in the periphery

CHIEN-CHUNG CHEN * and CHRISTOPHER W. TYLER
Smith-Kettlewell Eye Research Institute, 2318 Fillmore Street, San Francisco, CA 94122, USA

Received 10 June 1998; accepted 23 November 1998

Abstract—We measured the effect of phase coherence on the detectability of a chain of Gabor patches. The stimuli were elongated patterns consisting of 1–8 vertical Gabor patches, aligned vertically and either in phase or 180 deg out of phase from their immediate neighbors. In the fovea, the phase configuration had no effect on detection threshold, suggesting a full-wave rectification operation mediating foveal spatial summation. At 5 deg in the periphery, detection thresholds for the in-phase configuration were lower than those for the alternating-phase configuration, to an extent compatible with a half-wave rectification operation mediating peripheral spatial summation.

Keywords: Spatial summation; phase; fovea vs periphery; rectifier.

INTRODUCTION

Most current models of spatial vision mechanisms (e.g. Klein and Levi, 1985; Watt and Morgan, 1985; De Valois and De Valois, 1988; Sperling, 1989; Wilson *et al.*, 1990; Watson and Solomon, 1997; Chen *et al.*, 1997) assume that the first stage of visual information processing contains localized linear filters whose spatial sensitivity profile resembles those of simple cells in the striate cortex (Hubel and Wiesel, 1962, 1968; De Angelis *et al.*, 1993). Each linear filter analyzes a small portion of the whole visual field which, by analogy to the receptive fields of neurons, is called the perceptive field (Spillmann *et al.*, 1987). However, recent studies show that localized linear filters are inadequate to account for the performance on tasks such as texture discrimination (Sperling, 1989; Graham *et al.*, 1992; Wilson and Richards, 1992), contour integration (Field *et al.*, 1993), and lateral pattern masking (Polat and Sagi, 1993). It has been suggested that the visual system contains second-order mechanisms that can integrate the outputs of the localized linear filters (Adelson and Bergen, 1985; Watt and Morgan, 1985; Sperling, 1989; Wilson and

*To whom all correspondence should be addressed.

Richards, 1992; Graham *et al.*, 1992; Morgan and Tyler, 1995). Usually, the outputs of the first-order mechanisms are manipulated by a nonlinear transform before they feed into the second-order mechanisms.

Most reported experiments on second-order mechanisms focus on the study of 'complicated' or 'higher level' discrimination tasks. Detecting periodic patterns is a task that might be expected to be governed by the first-order mechanisms. We here report an experiment showing that the localized linear filters or the first-order mechanisms alone cannot even explain a phenomenon as simple as detecting elongated periodic patterns. We show that a nonlinear transform is required before the pattern detector sums information across space. The evidence further suggests that this nonlinear transform is different in the fovea and in the periphery.

Our approach is to measure how the detection threshold of a pattern stimulus changes with its spatial extent. Previous studies have shown that the detection threshold for a periodic pattern first decreases steeply as the spatial extent (usually defined as number of cycles) of that pattern increases to a critical extent and then little, if any, threshold decrement is observed as the spatial extent of the pattern further increases (Hoekstra *et al.*, 1974; Howell and Hess, 1978; Robson and Graham, 1981; Quinn and Lehmkuhle, 1983; Tootle and Berkley, 1983; Makela *et al.*, 1994). This threshold reduction effect has been interpreted to reflect the finite spatial extent of the first-order linear filters.

The response of a linear filter to a pattern is the inner product of the sensitivity profile of that filter and the intensity profile of the pattern. That is

$$R_j = \sum_x \sum_y S_j(x, y) \cdot I_k(x, y), \tag{1}$$

where R_j is the response of filter j to pattern k, S_j is the sensitivity profile of filter j and I_k is the intensity profile of pattern k. The linear filter sums information from everywhere within its perceptive field. Suppose a pattern matches the linear filter in spatial frequency, orientation and phase. For such a pattern lying within the perceptive field of the filter, the greater the spatial extent of this pattern, the more spatial summation occurs within the linear filter and in turn the greater is the sensitivity. Thus, the threshold decreases proportionately with the increment of the spatial extent of the pattern within the range of the filters (a slope of -1 on log-log coordinates). On the other hand, since a linear filter with finite spatial extent cannot respond to patterns outside its perceptive field, the part of the pattern lying outside the perceptive field makes no contribution to its response. Once the spatial extent of the pattern matches that of the linear filter, further extending the pattern adds little to the filter response. Therefore, virtually no more threshold reduction occurs when the pattern extends further than a critical amount.

This critical size, under the linear filter assumption, provides a chance to measure the spatial extent of the filters psychophysically. Researchers have used this idea not only to measure the size of linear filters but also try to determine their shape. For instance, Polat and Tyler (1997) measured how detection threshold for a Gabor

pattern changed with the elongation of the Gaussian envelope. They found that the detection threshold decreased substantially when the Gaussian envelope was elongated parallel to the bars but not when the envelope extended orthogonal to the bars. Polat and Tyler inferred that the shape of the perceptive fields of pattern detectors are elongated with about a 6-to-1 length to width ratio.

However, this type of study has a theoretical drawback. There are two different spatial summation processes that can occur during a detection task. First, as discussed above, if a pattern is smaller than the perceptive field of a filter, spatial summation occurs within the filter. Second, if a pattern stimulates more than one filter, the visual system may combine information from many relevant filters for detection. If the system combined information *linearly* from different filters within a finite region, the perceptive field of this combination would be indistinguishable from the perceptive field of a larger linear filter. Thus, it is impossible to determine if the detectability of a uniform pattern is based on the response of one large linear filter or on a linear summation of responses of multiple smaller linear filters. For instance, Polat and Tyler (1997) pointed out that instead of elongated pattern detectors, their data can also be interpreted as a linear combination of several collinear circular filters.

A nonlinear combination of linear filters will respond differently from a large linear filter to certain phase relations among the patterns, but this difference will not occur if the pattern detector combines information from local linear filters nonlinearly, i.e. the pattern detectors are second-order filters. To test this hypothesis, we alternated the phase of the pattern locally and observed how threshold changed with the spatial extent of the pattern. In most models of spatial vision, second-order mechanisms, analogous to the complex cells in visual cortex, are phase-insensitive. Thus, if the pattern detection is mediated by second-order mechanisms, the threshold should not be affected by changes in local phase among the micro-patterns.

METHODS

Equipment

The stimuli were presented on a SONY CPD-1425 monitor driven by a Radius PrecisionColor graphic board. A Macintosh Quadra Pro computer controlled the graphic board. The resolution of the monitor was 640 horizontal by 480 vertical pixels. At the viewing distance we used (128 cm), there were 60 pixels per degree. The viewing field was then 10.7 deg (H) by 8 deg (V). The refresh rate of the monitor was 60 Hz. We used the LightMouse photometer (Tyler, 1997) to measure the input-output intensity function of the monitor. This information allowed us to compute linear lookup table settings. The mean luminance of the monitor was set at 26 cd/m^2.

The experimental control software was written in MATLAB (MathWorks Inc., 1993) using the Psychophysics Toolbox (Brainard, 1997), which provides high level access to the C-language VideoToolbox (Pelli, 1997).

Stimuli

Each stimulus contained a chain of 1 to 8 vertical Gabor patches aligned vertically. Examples of the stimuli are shown in Fig. 1. Each Gabor patch is defined by

$$I(x, y) = C \cdot \cos(2\pi f x + \phi) \cdot \exp\left(-\frac{(x-u)^2}{2\sigma^2}\right) \cdot \exp\left(-\frac{(y-v)^2}{2\sigma^2}\right), \quad (2)$$

where C is the contrast, f is the spatial frequency, and ϕ is the phase of the cosinusoidal modulation, u is the horizontal distance and v is the vertical distance from the center of the Gabor patch to the fixation point, and σ is the scale parameter of the Gaussian envelope. In our experiment, the spatial frequency of the Gabor patches was 4 cycles per degree and the scale parameter was 0.0721 deg providing a modulation packet one cycle in width at half-amplitude, which is luminance balanced within 1%. The phase of a Gabor patch was either 0 deg or 180 deg relative to the center of the stimulus.

The distance between the centers of two neighboring Gabor patches was 6σ. That is, for the Gabor patch with $\sigma = 0.0721$ deg, the distance was 0.44 deg. The string of Gabors was always centered at the same point, meaning that there was a patch at the center of the string for odd numbers and a gap at the center for even numbers. For a stimulus containing an odd number of Gabor patches, the vertical distance from the center of each patch to the fixation point is defined as $v = \pm(k-1)\sigma$, $k = 1, 3, \ldots, n$ from the most central to the most peripheral Gabor patches and n is

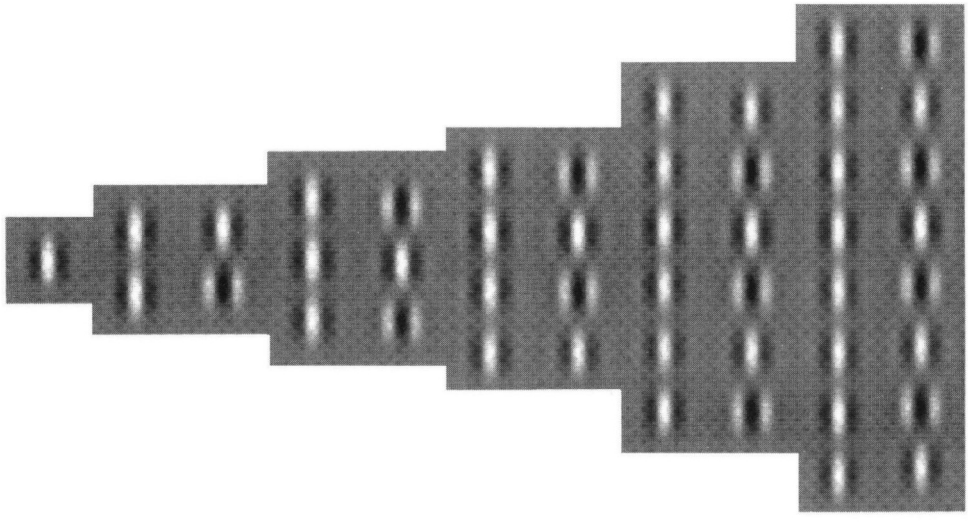

Figure 1. Samples of the in-phase and alternating-phase stimuli used in the experiments.

the number of patches. For a stimulus containing an even number of Gabor patches, $v = \pm 3(k-1)\sigma$, $k = 2, 4, \ldots, n$ from the most central to the most peripheral patches.

There were two phase configurations. In the in-phase configuration, all the Gabor patches were in phase with the center of the global stimulus. In the alternating-phase configuration, the phase of each patch was 180-degree out of phase from its immediate neighbors.

The threshold for each stimulus was measured under two viewing conditions. In the foveal viewing condition, the fixation point was at the center of the monitor, i.e. parameter u in equation (1) was set to zero. In the peripheral viewing condition, the fixation was placed 5 deg horizontally to the left of the center of the screen. Thus, with respect to the fixation point, parameter u was set to -5 deg.

There is concern about the possible influence of the cortical magnification factor on our peripheral results obtained with the same stimuli as in the fovea (Levi *et al.*, 1985). For a comparison, we also used cortically scaled stimuli in the periphery. The scaled stimuli had all dimensions expanded by 3-fold from the unscaled stimuli. That is, the 3-fold scaled Gabor patches had a spatial frequency 1.33 cycle per degree and a scale parameter 0.2163 deg. The distance between two Gabor patches remained at 60 and thus increased by 3-fold to 1.2978 deg. In addition, we used patches scaled by 7-fold in size and in separation. The 7-fold patch had a spatial frequency of 0.57 cycle per degree and a scale parameter of 0.5257 deg. The distance between two neighboring patches became 3.1542 deg.

Procedure

Detection thresholds were measured with a temporal two-alternative forced-choice (2AFC) paradigm where a target pattern was flashed for 100 ms randomly in one of the two intervals while the other showed only a uniform background at the mean luminance of the pattern. An 800 ms blank period separated the two intervals and a blank period of at least 1200 ms separated successive 2AFC trials. There were 40 trials in each threshold measurement. The placement of target contrast in each trial and the estimated threshold in each measurement were determined by the QUEST adaptive procedure (Watson and Pelli, 1983). The thresholds were measured at 91% correct level. The reported threshold of each target pattern was based on the average of 4 to 6 measurements.

There were three observers. CCC is an author of this article. JW and NCF were paid observers naïve to the purpose of the experiment. All observers had a corrected to normal visual acuity and were experienced in psychophysical experiments.

RESULTS

Foveal summation

Figure 2 shows the detection threshold as a function of the number of Gabor patches in a test stimulus. The closed circles denote the in-phase configuration while the open circles denote the alternating-phase configuration. The error bars in this and other figures of this paper show the standard error of measurements. The solid and dashed curves are the full-wave rectification model as fitted to the data for discussion later in the paper.

The detection thresholds for both in-phase and alternating-phase patterns are not significantly different for any number of Gabor patches. This suggests that phase has no effect on the detection of elongated patterns in the fovea. Detection threshold decreases substantially (3–4.6 dB) as the number of Gabor patches n increases from 1 to 2. Much less threshold reduction occurs as n increases from 2 to 3 and almost no further threshold reduction occurs as the number of Gabor patches is further increased. Note that the elongation of 6 : 1 found by Polat and Tyler (1997) would predict summation of a string of three Gabor patches.

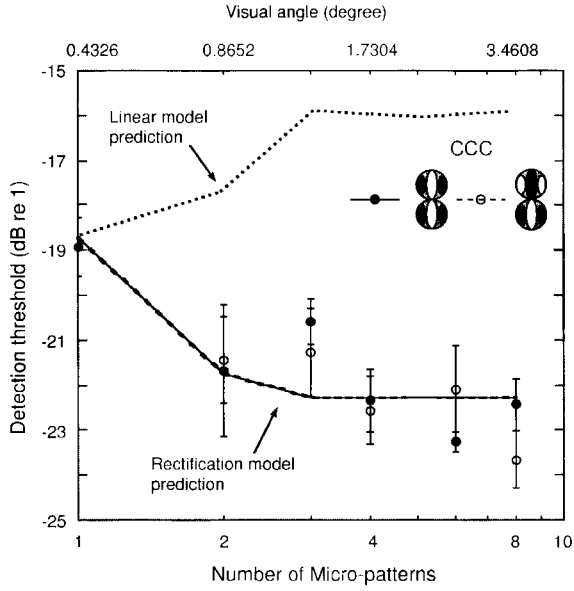

Figure 2. Detection thresholds in the fovea as a function of the number of Gabor patches. Panels (a) to (c) show data for three observers. In each panel, the closed circles denote the in-phase configuration while the open circles denote the alternating-phase configuration. The solid and broken curves are full-wave rectification model fits to in-phase and alternating data respectively. The y-axis is the detection threshold in dB. The x-axis is the number of Gabor patches. We also put the visual angle on the x-axis for comparison. The visual angle is measured as the distance from the 3σ on one side of the Gabor patch to the 3σ on the other. The model fits to the two data sets are indistinguishable in this figure. The bold dotted curves are the best linear model fits to the alternating-phase condition. The error bars are the standard error of each set of measurements.

Data from one observer (NCF) do show a visible difference between the in-phase and alternating-phase configurations (Fig. 2c). We tried to fit two sets of data with different parameters in the model. The sum of squared error did improve with the number of parameters but not significantly ($F(1, 9) = 5.3513$, $p = 0.046 > 0.01$). A t-test on the difference of thresholds at the greatest spatial extent of the stimuli (containing eight Gabor patches each) also showed no statistically significant difference ($t(6) = 2.1896$, $p = 0.036 > 0.01$).

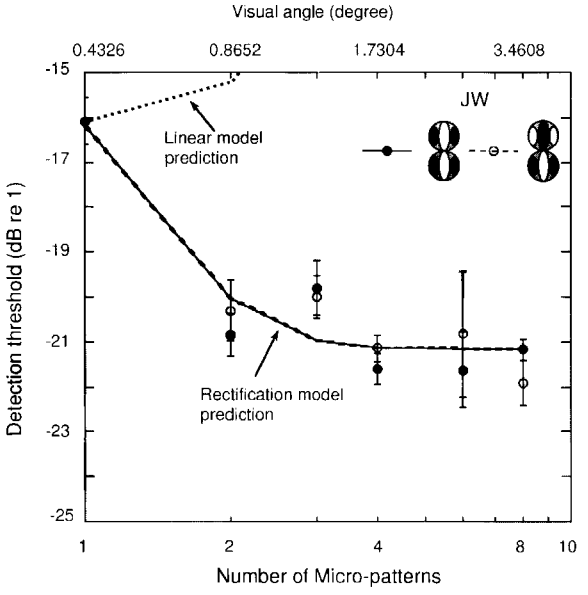

(b)

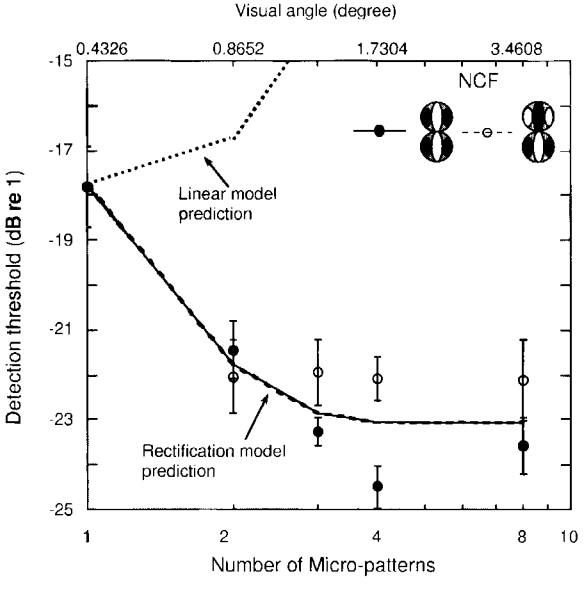

(c)

Figure 2. (Continued).

The bold dotted curve shows the linear filter prediction to the alternating phase data based on the fit of the optimal size for the in-phase condition. Even if we further optimize the location of the filter for best fit to the alternating-phase data, the linear prediction still shows a dramatic mismatch for the alternating phase condition. Details of the derivation of linear filter response are given in the Appendix.

Peripheral summation

The phase effect on spatial summation in the periphery is very different from that in the fovea. Figure 3 shows the detection threshold for unscaled test patterns at the 5 deg peripheral location. The closed circles denote the in-phase configuration while the open circles denote the alternating-phase configuration. The model curve will be discussed later in the next section.

Threshold for the in-phase configuration dropped rapidly by 6–9 dB (about a factor of two to three increase in sensitivity) as the number of Gabor patches increased from 1 to 4 while, in the same range, the threshold for the alternating-phase configuration dropped only about 3 dB. Thus, there was more spatial summation for the in-phase than for the alternating-phase configuration. Even more interesting is that, for n larger than 2, the threshold for an alternating-phase pattern with $2 \cdot n$ Gabor patches was about the same as the threshold for an in-phase pattern with n Gabor patches. In terms of the linear/nonlinear filter hypotheses commonly

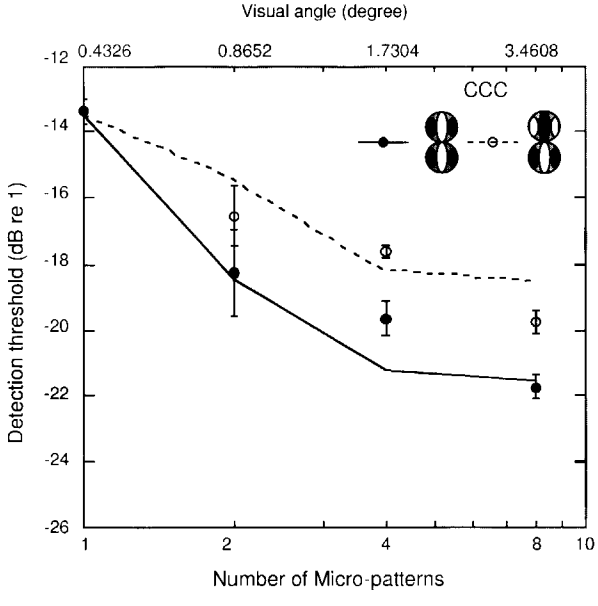

(a)

Figure 3. Detection thresholds at 5 deg in the periphery as a function of the number of Gabor patches, unscaled for eccentricity. Panels (a) to (c) show data for three observers. In each panel, the closed circles denote the in-phase configuration while the open circles denote the alternating-phase configuration. The solid and broken curves are half-wave rectification model fits to the in-phase and alternating-phase data, respectively.

used in vision, this result suggests that a half-wave rectification operation on linear-filter responses is involved in spatial summation and pattern detection.

Figure 4 shows the data for stimuli scaled up by a factor of three at the same location in the periphery to match the cortical scaling factor for pattern detection (Levi *et al.*, 1985). The pattern of results is not very different from that for the unscaled stimuli except the overall sensitivity increases by a factor of about

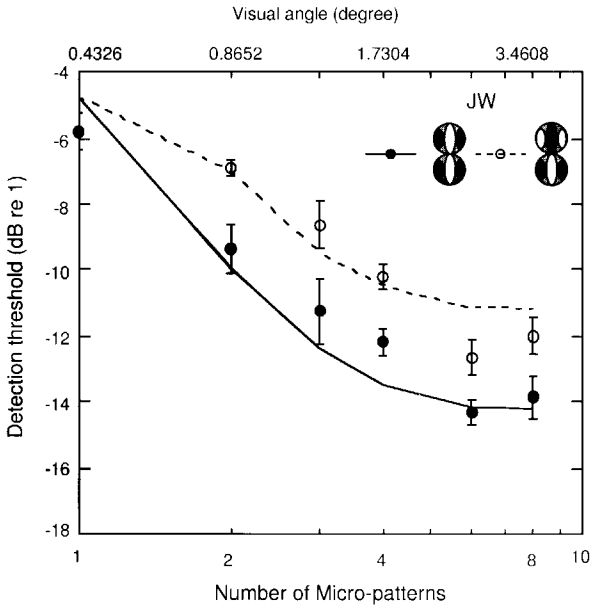

(b)

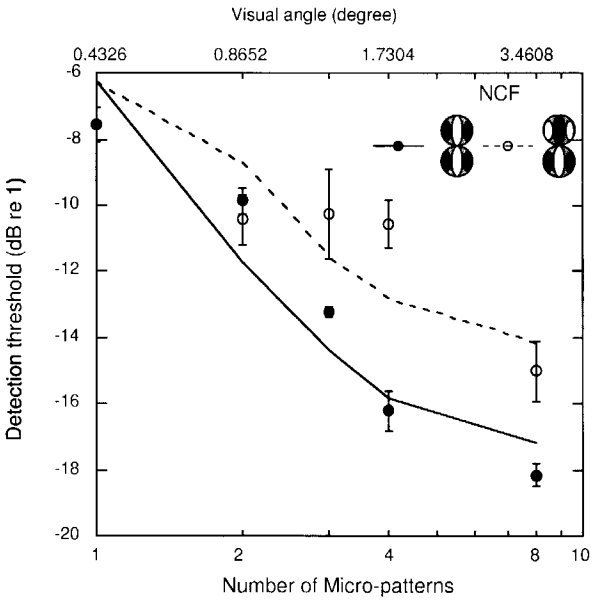

(c)

Figure 3. (Continued).

5 (14 dB), bringing it up to and beyond the level of foveal sensitivity. Even at this size, summation still extends over 2–4 micropattern separations and the difference between phase conditions becomes larger rather than smaller. Thus, the cortical magnification factor does not explain the distinct difference in phase effects in the foveal and in the peripheral regions.

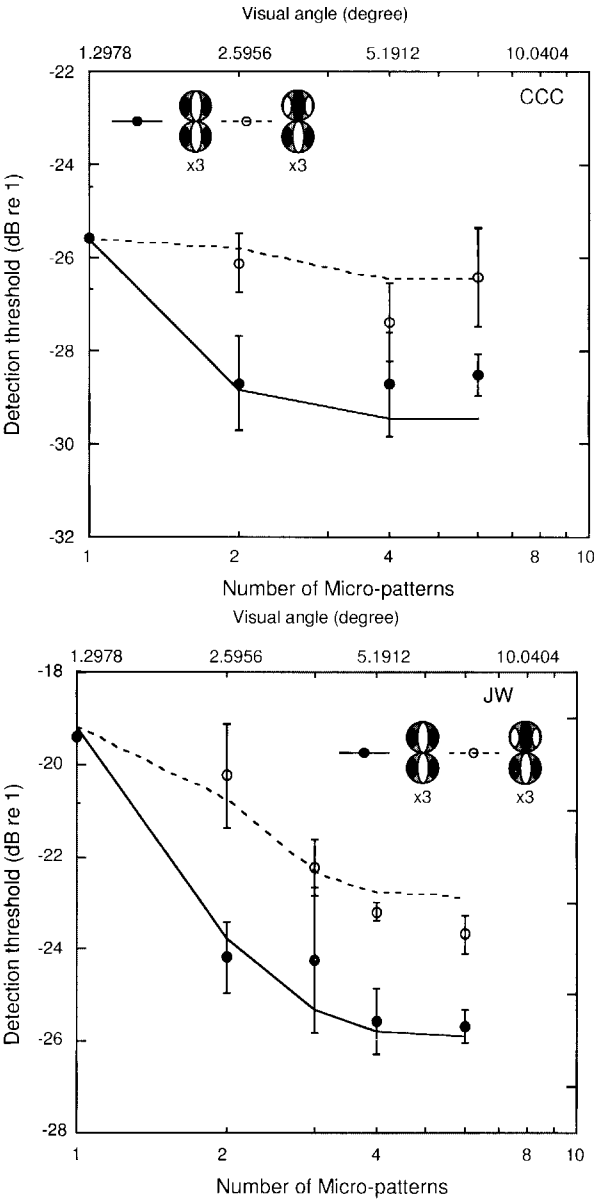

Figure 4. Detection thresholds at 5 deg eccentricity as in Fig. 3 but with 3-fold eccentricity scaled stimuli. Observer NCF was not available for this condition.

Although a cortical magnification factor of 3 at 5 deg eccentricity is appropriate for Gabor pattern detection (Levi *et al.*, 1985), studies using Vernier acuity tasks showed a greater cortical magnification factor — in some estimations, the magnification factor can be up to 7 (Beard *et al.*, 1997). The difference in the cortical magnification factors may result in a dispute of which scaling factor we should use when we move the stimuli from fovea to 5 deg at the periphery. Although estimating the correct cortical magnification factor is not a purpose of this paper, we nevertheless ran a control experiment to show that the difference in the scaling factors has no effect on the conclusions we want to draw about the difference in detecting in-phase and alternating-phase configurations.

We enlarged the unscaled pattern by 7-fold in all dimensions, presented at the same 5 deg peripheral location. Due to the size of the stimuli, this experiment was done on a different host machine (Apple PowerPC 8100) with a bigger monitor (NEC XE17) than the system we used for the main experiments. Accompanying the hardware change, the thresholds were measured with the PSI adaptive procedure (Kontsevich and Tyler, in press) at the 75% performance level rather than at 91% level in the main experiments. The difference in the percentage of correct level reflects the optimal operational level of the two adaptive methods.

Figure 5 shows the data of observer CCC for stimuli scaled up by a factor of seven. The pattern of results is again similar to those for the unscaled and 3-fold enlarged stimuli in Figs 3a and 4a except the thresholds are much lower than in the fovea. Thus, the cortical magnification factor does not explain the distinct difference in

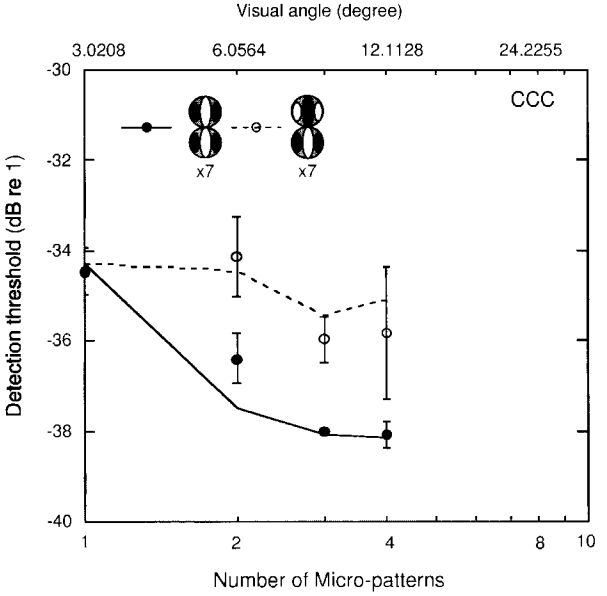

Figure 5. Detection thresholds at 5 deg eccentricity as in Fig. 3 but with 7-fold eccentricity scaled stimuli.

phase effects in the foveal and in the peripheral regions. The choice of cortical magnification factor does not seem to be an important issue in our experiment.

MODELS

The data show that pattern detection behavior in the fovea is very different from that at 5 deg in the periphery. The phase configuration of the stimuli has no significant effect on pattern detection in the fovea. This suggests that the visual system uses an operation such as full-wave rectification to discard the phase polarity information in the stimulus. Figure 6 shows a model that implements this operation and quantitatively accounts for the threshold reduction as the number of Gabor patches increases. The input stimulus is first processed by a series of localized linear filters, but there is no direct output from these filters to the perceptual decision stage. For convenience of computation, we set the size, location, spatial frequency, and orientation of the linear filters commensurate with the Gabor patches. At each location, there are two such linear filters each with opposite phase from the other. The response of each linear filter is defined by equation (1). For the Gabor patches we use (see equation (2)), the response of each filter can be obtained by substituting $I(x, y)$ in equation (1) by equation (2) and can be simplified as

$$R(x, y) = S_e \cdot C, \tag{3}$$

where C is the contrast of the Gabor patch and S_e is the inner product of the Gabor function and the sensitivity profile of the linear filter. The value of S_e is a constant for all filters and its sign is determined by the phase of the linear filter. We define S_e to be positive for in-phase filters and negative for 180-degree out-of-phase filters. S_e thus represents the sensitivity to a stimulus patch.

The response of each linear filter is half-wave rectified and feeds to the same summation mechanism. The combination of two half-wave rectified linear filter responses is equivalent to a full-wave rectified linear filter output. The reason for

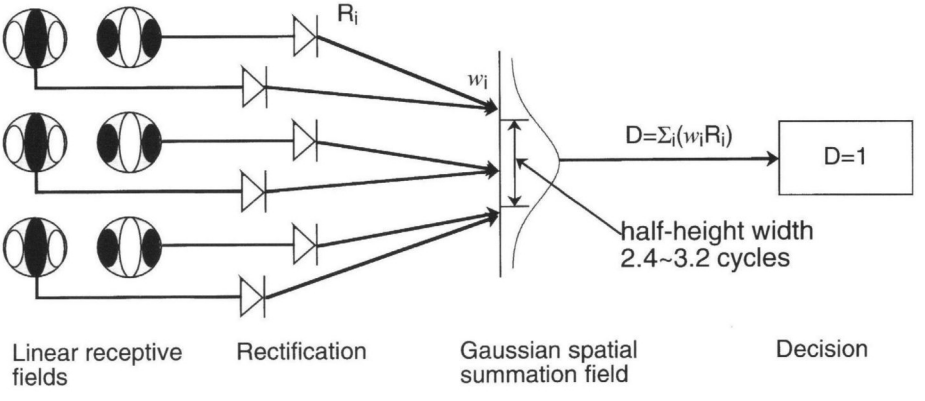

Figure 6. A diagram illustrating the full-wave rectification model. See text for details.

separating the two half-wave rectified linear filter banks is to be consistent with the results from phase discrimination studies (Atkinson and Campbell, 1974; Nachmias and Weber, 1975; Lawden, 1983) and phase effects on pattern masking (Bowen, 1995; Foley and Chen, in press). The summation mechanism has a summation field defined by a Gaussian function. The response of each linear filter is weighted by this Gaussian function. This is,

$$w_i = \exp\left(-\frac{d_i^2}{2\sigma^2}\right), \tag{4}$$

where w_i is the weight applying to the i-th linear filter, d_i is the distance from the center of the i-th filter to the center of the summation field and σ is the scale parameter of the Gaussian function. The decision variable D is the weighted sum of rectified linear filter responses. That is,

$$D = \sum_i [w_i \cdot R]. \tag{5}$$

The fit of the model is shown in Fig. 2. The root of the mean squared error (RMSE) of the model fit was between 0.59 and 0.81 dB for the three observers, not significantly greater than the standard error of measurement (0.57 to 0.75 dB). The values of the parameters are shown in Table 1. The scale parameter of the Gaussian summation field σ was about 0.26 deg to 0.32 deg corresponding to half-height length of 2.44 to 3.0 cycles. These values are slightly lower than these reported by Polat and Tyler (1997).

The detection behavior at 5 deg in the periphery is qualitatively different from that in the fovea. The difference in magnitudes of threshold reduction for in-phase and alternating-phase configurations suggests a half-wave rectification operation. To account for this data set, we make a simple modification on the full-wave rectification model discussed above. This model is shown in Fig. 7. Instead of feeding the rectified response into the same summation mechanisms, linear filters with different phase preferences feed into separate summation mechanisms. To constrain the number of free parameters, we assume these two summation

Table 1.
The resulting model fits to the combined data set in foveal viewing conditions. The parameter S_e is the contrast sensitivity defined in equation (3) and σ is the scale parameter of the summation field defined in equation (4). RMSE indicates the goodness-of-fit. We also show σ as the half-height width of the Gaussian summation field in cycles of the Gabor stimulus for the purpose of comparison

	Contrast sensitivity S_e	Scale parameter σ (deg)	Half-height width (cycle)	RMSE (dB)
CCC	8.6484	0.2598	2.44	0.7625
JW	6.4772	0.3060	2.88	0.5919
NCF	7.7321	0.3175	3.00	0.8162

mechanisms occupy the same location and have the same spatial extent. The receptive field of this summation mechanism is defined by a Gaussian function. The output of j-th summation field, O_j, is the weighted sum of half-wave rectified linear filter outputs as defined by equations (4) and (5). The decision variable assumes a quadratic pooling of two summation mechanism outputs

$$D = \left(O_1^2 + O_2^2\right)^{0.5}. \tag{6}$$

The fits of the model are shown in Fig. 3 for unscaled stimuli and in Figs 4 and 5 for scaled stimuli. The RMSE of the model fit is between 0.50 to 0.87 dB for CCC and JW for both scaled and unscaled data set. The RMSEs for the two observers are very close to the standard error of measurements (0.54 to 0.87 dB). The RMSE

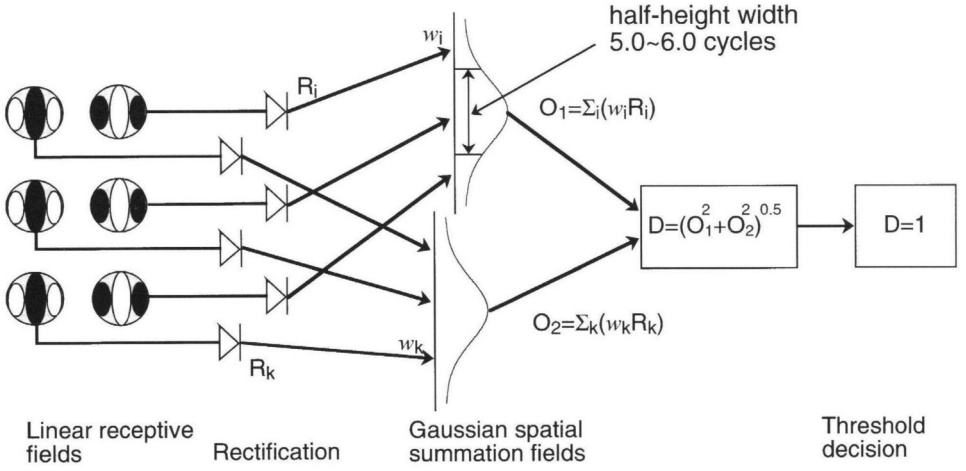

Figure 7. A diagram illustrating the half-wave rectification model. See text for details.

Table 2.
The resulting model fits to combined data set in peripheral viewing conditions. The parameter S_c is the contrast sensitivity defined in equation (3) and s is the scale parameter of the summation field defined in equation (4). RMSE indicates the goodness-of-fit. We also show σ as the half-height width of the Gaussian summation field in cycles of the Gabor stimulus for the purpose of comparison

	Contrast sensitivity S_c	Scale parameter σ (deg)	Half-height width (cycle)	RMSE (dB)
Unscaled				
CCC	2.0494	0.4369	4.12	0.8360
JW	1.7289	0.5126	4.92	0.8819
NCF	4.7230	0.6104	5.76	1.3591
Scaled				
CCC	19.0603	0.8078	2.54	0.5076
JW	9.1161	1.1185	3.52	0.7056

for the NCF data set is as high as 1.35 dB while the standard error of measurement is 0.62 dB. However, his data also shows more irregularity than the other observers. The values of the parameters are shown in Table 2. The scale parameter σ increases by 70–300%, indication that peripheral length summation is more extensive than in the fovea.

DISCUSSION

No linear filter can account for the pattern of the data across phase conditions. We have shown above (Fig. 2) that the linear filters that account for in-phase data cannot explain the alternating-phase data. There is another possibility, that the threshold reduction for alternating-phase configuration reflects off-orientation looking with linear filters. The notion is that an alternating-phase stimulus looks somewhat like a checkerboard. A two-dimensional Fourier transform shows that there is contrast energy peaking at 29 deg off the vertical axis in the power spectrum. Thus, it is possible that a tilted linear filter rather than a vertical one could mediate the detection of an alternating-phase stimulus and that the threshold reduction for the alternating-phase configuration only reflects the spatial summation in this tilted filter. We approached this problem by computing how much improvement we could get by tilting the linear filters. We optimized the orientation, spatial frequency, and phase of the filter for detecting each individual alternating-phase stimulus. The size of the isotropic filter was determined by the best fit to in-phase data. We found that the tilted filter could improve the threshold by 2.14 dB as the number of Gabor patches increased from 1 to 2 while our alternating-phase results gave 3 to 4.6 dB improvement. Thus, quantitatively, off-orientation looking cannot be the decisive factor in our results.

Figure 2 shows that spatial summation for detection of elongated stimuli in the fovea is insensitive to phase. Field *et al.* (1993) and Hess and Dakin (1997) reported a similar phase insensitivity in their suprathreshold contour integration paradigm. In contour integration experiments, the task of an observer is to extract a contour consisting of several suprathreshold Gabor micro-patterns among otherwise randomly scattered and oriented micro-patterns. The phase relationship among micro-patterns in a contour did not substantially affect on the ability of an observer to integrate suprathreshold patterns across different spatial locations. In a different paradigm, Dresp and Grossberg (1997) observed the effect of a subthreshold thin line on illusory contours and showed that any luminance polarity of the thin line could equally enhance the illusory contour induced by inducing lines in any luminance polarity. These converging lines of evidence indicate that there must be phase-insensitive spatial summation mechanisms in our visual system. The present data show that such phase-insensitive mechanisms operate all the way down to detection threshold in the fovea.

We also show that there is a qualitative difference between foveal and peripheral vision in processing phase information. This result is also consistent with earlier

reports with other paradigms (Rentschler and Treutwein, 1985; Bennett and Banks, 1987, 1991; Hess and Pointer, 1987; Stephenson *et al.*, 1991; Hess and Dakin, 1997). For example, Hess and Dakin (1997) reported that in the periphery their observers had a much greater difficulty in a contour integration task in extracting a contour that contained elements alternating in phase than one that contained only in-phase elements. They did not observe the same effect in the fovea. Thus, it is more difficult for the spatial summation mechanisms in the peripheral to integrate information across different phases.

It may seem paradoxical that our summation results show phase insensitivity in the fovea while phase discrimination in the fovea is better than that in the periphery (Rentschler and Treutwein, 1985; Bennett and Banks, 1987, 1991; Hess and Pointer, 1987; Stephenson *et al.*, 1991). However, as shown above, the phase insensitivity of spatial summation occurs when a summation mechanism pools responses from linear filters with different phase preferences. As a result, the local phase information is lost. This loss of local phase information in second-order mechanisms has been reported in texture discrimination studies (Caelli and Bevan, 1982). On the other hand, phase discrimination thresholds are measured by comparing two patterns with different phase compositions that result different responses in one or more filters. The phase preference and phase tuning of the linear filters determine phase discrimination. Thus, to perform a phase discrimination task, the visual system must be able to read the outputs from each individual linear filter (Tyler and Gorea, 1986). This requires a different decision mechanism than the one proposed in this article. Since this phase discrimination task requires local read-out mechanisms and different perceptual decision mechanisms from pattern summation, the implication of this local read-out is that the phase discrimination involved no spatial summation and would be predicted to be invariant with the size of the stimuli.

REFERENCES

Adelson, E. H. and Bergen, J. (1985). Spatio-temporal energy models for the perception of motion, *Journal of the Optical Society of America A* **2**, 284–299.

Atkinson, J. and Campbell, F. W. (1974). The effect of phase on perception of compound gratings, *Vision Research* **14**, 159–162.

Beard, B. L., Levi, D. M. and Klein, S. A. (1997). Vernier acuity with non-simultaneous targets: The cortical magnification factor estimated by psychophysics, *Vision Research* **37**, 325–346.

Bennett, P. J. and Banks, M. S. (1987). Sensitivity loss in odd-symmetric mechanisms and phase anomalies in peripheral vision, *Nature* **326**, 873–876.

Bennett, P. J. and Banks, M. S. (1991). The effects of contrast, spatial scale, and orientation on foveal and peripheral phase discrimination, *Vision Research* **31**, 1759–1786.

Bowen, R. W. (1995). Isolation and interaction of ON and OFF pathways in human vision: pattern polarity effects in contrast discrimination, *Vision Research* **35**, 2479–2490.

Brainard, D. H. (1997). The psychophysics toolbox, *Spatial Vision* **10**, 433–436.

Caelli, T. and Bevan, P. (1982). Visual sensitivity to two-dimensional spatial phase, *Journal of the Optical Society of America* **72**, 1375–1381.

Chen, C. C., Foley, J. M. and Brainard, D. H. (1997). Detection of chromatic patterns on chromatic pattern pedestals, *IS and T Proceedings: Optics and Imaging in the Information Age* 19–24.

De Angelis, G. C., Ohzawa, I. and Freeman, R. D. (1993). Spatiotemporal organization of simple-cell receptive fields in the cat's striate cortex. I. General characteristics and postnatal development, *Journal of Neurophysiology* **69**, 1091–1117.

De Valois, R. L. and De Valois, K. K. (1988). *Spatial Vision*. Oxford University Press, Oxford.

Dresp, B. and Grossberg, S. (1997). Contour integration across polarities and spatial gaps: from local contrast filtering to global grouping, *Vision Research* **37**, 913–924.

Field, D. J., Hayes, A. and Hess, R. F. (1993). Contour integration by the human visual system: evidence for a local 'association field', *Vision Research* **33**, 173–193.

Foley, J. M. and Chen, C. C. (1999). Pattern detection in the presence of maskers that differ in spatial phase and temporal offset; threshold measurements and a model, *Vision Research* (in press).

Graham, N., Beck, J. and Sutter, A. (1992). Nonlinear processes in spatial frequency channel models of perceived texture segregation, *Vision Research* **32**, 719–743.

Hess, R. F. and Pointer, J. S. (1987). Evidence for spatially local computations underlying discrimination of periodic patterns in fovea and periphery, *Vision Research* **27**, 1343–1360.

Hess, R. F. and Dakin, S. C. (1997). Absence of contour linking in peripheral vision, *Nature* **390**, 602–604.

Hockstra, J., van der Goot, D. P. J., van den Brink, G. and Bilsen, F. A. (1974). The influence of the number of cycles upon the visual contrast threshold for spatial sine wave patterns, *Vision Research* **14**, 265–268.

Howell, E. R. and Hess, R. F. (1978). The functional area for summation to threshold for sinusoidal gratings, *Vision Research* **18**, 369–374.

Hubel, D. H. and Wiesel, T. N. (1962). Receptive fields, binocular interaction and functional architecture in the cat's visual cortex, *Journal of Physiology* **160**, 106–154.

Hubel, D. H. and Wiesel, T. N. (1968). Receptive fields and functional architecture of monkey striate cortex, *Journal of Physiology* **195**, 215–243.

Klein, S. A. and Levi, D. M. (1985). Hyperacuity thresholds of 1.0 second: theoretical predictions and empirical validation, *Journal of the Optical Society of America A* **2**, 1170–1190.

Kontsevich, L. L. and Tyler, C. W. Baysian adaptive estimation of psychometric slope and threshold, *Vision Research* (in press).

Lawden, M. C. (1983). An investigation of the ability of the human visual system to encode spatial phase relationships, *Vision Research* **23**, 1451–1453.

Levi, D. M., Klein, S. A. and Aitsebaomo, A. P. (1985). Vernier acuity, crowding and cortical magnification, *Vision Research* **35**, 963–977.

Makela, P., Rovamo, J. and Whitaker, D. (1994). Effects of luminance and external temporal noise on flicker sensitivity as a function of stimulus size at various eccentricities, *Vision Research* **34**, 1981–1991.

MathWorks (1993). *MATLAB*. The MathWorks Inc., Natick.

Morgan, M. J. and Tyler, C. W. (1995). Mechanisms for dynamic stereomotion respond selectively to horizontal velocity components, *Proceedings of the Royal Society of London series B, Biological Science* **262**, 371–376.

Nachmias, J. and Weber, A. (1975). Discrimination of simple and complex gratings, *Vision Research* **15**, 213–217.

Pelli, D. G. (1997). The Video Toolbox software for visual psychophysics: transform numbers into movies, *Spatial Vision* **10**, 437–442.

Polat, U. and Sagi, D. (1993). Lateral interactions between spatial channels: suppression and facilitation revealed by lateral masking experiments, *Vision Research* **33**, 993–999.

Polat, U. and Tyler, C. W. (1997). What pattern the eye sees best, *Investigative Ophthalmology and Visual Science (Suppl.)* **38**, 1.

Quinn, P. C. and Lehmkuhle, S. (1983). An oblique effect of spatial summation, *Vision Research* **23**, 655–658.

Rentschler, I. and Treutwein, B. (1985). Loss of spatial phase relationship in extrafoveal vision, *Nature* **313**, 308–310.

Robson, J. G. and Graham, N. (1981). Probability summation and regional variation in contrast sensitivity across the visual field, *Vision Research* **21**, 409–418.

Sperling, G. (1989). Three stages and two systems of visual processing, *Spatial Vision* **4**, 183–207.

Spillmann, L., Ransom-Hogg, A. and Oehler, R. (1987). A comparison of perceptive and receptive fields in man and monkey, *Human Neurobiology* **6**, 51–62.

Stephenson, C. M., Knapp, A. J. and Braddick, O. J. (1991). Discrimination of spatial phase shows a qualitative difference between foveal and peripheral processing, *Vision Research* **31**, 1315–1326.

Tootle, J. S. and Berkley, M. A. (1983). Contrast sensitivity for vertically and obliquely oriented gratings as a function of grating area, *Vision Research* **9**, 907–910.

Tyler, C. W. (1997). The Morphonome image psychophysics software and a calibrator for Macintosh systems, *Spatial Vision* **10**, 479–484.

Tyler, C. W. and Gorea, A. (1986). Different encoding mechanisms for phase and contrast, *Vision Research* **26**, 1073–1082.

Watson, A. B. and Solomon, J. S. (1997). Model of visual contrast gain control and pattern masking, *Journal of the Optical Society of America A* **14**, 2379–2391.

Watson, A. B. and Pelli, D. G. (1983). Quest: A Bayesian adaptive psychometric method, *Perception and Psychophysics* **33**, 113–120.

Watt, R. J. and Morgan, M. J. (1985). A theory of the primitive spatial code in human vision, *Vision Research* **25**, 1661–1674.

Wilson, H. R. and Richards, W. A. (1992). Curvature and separation discrimination at texture boundaries, *Journal of the Optical Society of America A* **9**, 1653–1662.

Wilson, H. R., Levi, D., Maffei L., Rovamo, J. and De Valois, R. (1990). The perception of form: Retina to striate cortex, in: *Visual Perception: The Neurophysiological Foundations*, L. Spillmann and J. S. Werner (Eds), pp. 231–272.

APPENDIX: DERIVING THE BEST LINEAR PREDICTIONS ON ALTERNATING-PHASE DATA

Assume that the best linear filter that accounts for our data has a Gabor sensitivity profile with width, orientation and spatial frequency matching the individual Gabor patches. This linear filter differs from the Gabor patches only in length and location. The length of the linear filter is specified by the scale parameter (standard deviation) of the Gaussian envelope. Since the same linear filter has to be able to account for both the in-phase and alternating-phase data, its scale parameter can be determined by the best fit to the in-phase data. Suppose the center of a Gabor patch is shifted away from the center of the linear filter by u degree. The response of the linear filter to this Gabor patch is

$$R = a \cdot \int \left\{ \exp\left[-\frac{(y-u)^2}{2\sigma_p^2} \right] \cdot \exp\left[-\frac{y^2}{2\sigma_f^2} \right] \right\} dy$$

$$= b \cdot \left(\frac{\sigma_p^2 \sigma_f^2}{\sigma_p^2 + \sigma_f^2} \right)^{0.5} \cdot \exp\left[-0.5 \cdot \frac{u^2}{\sigma_p^2 + \sigma_f^2} \right], \qquad \text{(A1)}$$

where a and b are constants, and σ_p and σ_f are scale parameters for the Gabor patch and the filter respectively.

The response of the linear filter to a two-Gabor patch stimulus is the response to the in-phase pattern summed with a negative, shifted pattern for the 180-degree out-of-phase element.

$$R = b \cdot \left(\frac{\sigma_p^2 \sigma_f^2}{\sigma_p^2 + \sigma_f^2} \right)^{0.5} \times \left\{ \exp\left[-0.5 \cdot \frac{u^2}{\sigma_p^2 + \sigma_f^2} \right] - \exp\left[-0.5 \cdot \frac{(u + 6\sigma_p)^2}{\sigma_p^2 + \sigma_f^2} \right] \right\}. \quad \text{(A2)}$$

The optimal distance between the linear filter and the Gabor patches can be found by taking the derivative of equation (A2). The maximum response of the linear filter can be found by inserting the optimal distance back in to equation (A2). The threshold is 1/response. Similar computations can be made for stimulus with more than two Gabor patches.